

Boraguanidates: Synthesis, X-ray Structures, and Reactions of $\{\text{Li}_2[\text{Pr}_2\text{NB}(\text{NDipp})_2]\}_2$ with p-Block and Group 12 Element Halides

Andrea M. Corrente and Tristram Chivers*

Department of Chemistry, University of Calgary, Calgary, Alberta T2N 1N4, Canada

Received July 17, 2008

The new Dipp-substituted boranes (Dipp = 2,6-diisopropylphenyl) $\text{Pr}_2\text{NB}(\text{NHDipp})_2$ (**5**), $\text{BrB}(\text{NHDipp})_2$ (**7b**), and $\text{B}(\text{NHDipp})_3$ (**8**) have been prepared in high yields and characterized in solution by multinuclear NMR spectroscopy (^1H , ^{11}B and ^{13}C) and in the solid state by X-ray crystallography. Reaction of **5** with 2 equiv of $^n\text{BuLi}$ in *n*-hexane produces $\{\text{Li}_2[\text{Pr}_2\text{NB}(\text{NDipp})_2]\}_2$ (**6**) the first example of a stable dilithiated boraguanidate. The unsolvated complex **6** has a dimeric structure in the solid state. A survey of the reactions of **6** with p-block and Group 12 element halides revealed various types of reactivity including (a) disproportionation (InCl), (b) reduction to the metal (PbCl_2 , CdCl_2 , TeBr_4 , TeI_4 , and TlCl), and (c) simple metathesis (GeCl_2 , MgCl_2 , and ZnCl_2). The metathetical products were characterized by multinuclear NMR spectra but, in contrast to the dilithiated complex **6**, they readily decompose in non-coordinating solvents to form the diprotonated compound **5**.

Introduction

Amidates (**1**) and guanidates (**2**) are monoanionic ligands that have been extensively investigated as main-group and transition-metal complexes.¹ Both types of ligands have been incorporated into transition-metal catalysts, and they have also found use in materials applications such as atomic layer deposition.¹ Another notable feature is their ability to stabilize reactive metal centers. For example, the first amido indium hydride incorporated the sterically bulky *N,N'*-(2,6-diisopropylphenyl)formamidinate.² More recently, novel Au(II) complexes that are stable as solids at room temperature were prepared by using *N,N'*-(2,6-dimethylphenyl)formamidinate.³ Thermally stable Ge(I) dimers have also been isolated by employing either bulky amidinate or guanidinate ligands.⁴ Guanidates have also been found to stabilize high oxidation state molybdenum species,⁵ low coordinate yttrium,⁶ and low oxidation state gallium.⁷ Cationic, base-free

zirconium(IV) species have also been isolated.⁸ Jones and co-workers reported the synthesis and characterization of the first example of a Mg(I) complex containing the guanidate $[(\text{Dipp})\text{NC}(\text{N}^i\text{Pr}_2)\text{NDipp}]^-$, where Dipp = 2,6-diisopropylphenyl.⁹ X-ray crystallographic analysis of this complex revealed a unique example of a Mg–Mg single bond, an exciting development in the area of metal–metal bonding that illustrates impressively the ability of guanidate ligands to stabilize highly reactive species. More recently, the Jones group has demonstrated that both bulky amidates and guanidates can be employed to isolate thermally stable lead(II)¹⁰ and germanium(II)¹¹ complexes. In addition, variation of the R groups on the carbon atom of the ligand backbone has been shown to influence both the oxidation state of the metal and the coordination mode of group 13 guanidate complexes.¹² Rigid guanidate-type ligands

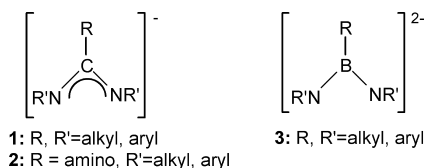
* To whom correspondence should be addressed. E-mail: chivers@ucalgary.ca. Phone: (403) 220-5741. Fax: (403) 289-9488.

- (1) For a recent review, see. Edelmann, F. T., *Adv. Organomet. Chem.*, **2008**, *57*, 183.
- (2) Baker, R. J.; Jones, C.; Junk, P. C.; Kloth, M. *Angew. Chem., Int. Ed.* **2004**, *43*, 3852.
- (3) Abdou, H. E.; Mohamed, A. A.; Fackler, J. P., Jr. *Inorg. Chem.* **2007**, *46*, 9692.
- (4) Green, S. P.; Jones, C.; Junk, P. C.; Lippert, K.-A.; Stasch, A. *Chem. Commun.* **2006**, 3978.
- (5) Cotton, F. A.; Daniels, L. M.; Murillo, C. A.; Timmons, D. J.; Wilkinson, C. C. *J. Am. Chem. Soc.* **2002**, *124*, 9249.

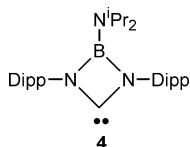
- (6) Trifonov, A. A.; Lyubov, D. M.; Fedorova, E. A.; Fukin, G. K.; Schumann, H.; Mühle, S.; Hummert, M.; Bochkarev, M. N. *Eur. J. Inorg. Chem.* **2006**, 747.
- (7) Jones, C.; Junk, P. C.; Platts, J. A.; Stasch, A. *J. Am. Chem. Soc.* **2006**, *128*, 2206.
- (8) Duncan, A. P.; Mullins, S. M.; Arnold, J.; Bergman, R. G. *Organometallics* **2001**, *20*, 1808.
- (9) Green, S. P.; Jones, C.; Stasch, A. *Science* **2007**, *318*, 1754.
- (10) Stasch, A.; Forsyth, C. M.; Jones, C.; Junk, P. C. *New J. Chem.* **2008**, *32*, 829.
- (11) Jones, C.; Rose, R. P.; Stasch, A. *Dalton Trans.* **2008**, 2871.
- (12) Jin, G.; Jones, C.; Junk, P.; Stasch, A.; Woodul, W. D. *New J. Chem.* **2008**, *32*, 835.

have been used to prepare tetranuclear Au(I) and dinuclear Au(II) complexes¹³ and to provide the first examples of structurally characterized B(II) monocations.¹⁴

In comparison to the carbon-based ligands, studies of the isoelectronic boraamidinate (*bam*) ligands (**3**) are limited.¹⁵ The introduction of a boron center into the ligand framework results in a dianionic charge that leads to unique reactivity. For example, stable spirocyclic radicals containing both the monoanionic radical, $[\text{PhB}(\text{N}^t\text{Bu})_2]^\bullet$ and the dianion $[\text{PhB}(\text{N}^t\text{Bu})_2]^{2-}$ *N,N'*-chelated to a group 13 center have been isolated.¹⁶ Complexes containing a *bam* ligand can also display unique bonding modes as evidenced by a recent investigation of heavy group 15 *bam* derivatives.¹⁷



As with amidinates and guanidinates, the steric and electronic properties of *bam* ligands can be tuned by varying the substituents at both boron and nitrogen. However, to the best of our knowledge, the only *bam* ligand that does not have an alkyl or aryl group on boron is the all-phenyl derivative $\text{Li}_2[\text{Ph}_2\text{NB}(\text{NPh})_2]$, which was found to eliminate LiNPh_2 in the presence of pyridine or dimethoxyethane (DME).¹⁸ In contrast to the decomposition of this dilithio derivative, Bertrand and co-workers have described the synthesis of **4**,¹⁹ in which a carbene center is stabilized in a four-membered ring by a boraguanidinate (*bog*) ligand;²⁰ electron donation from the $-\text{N}^i\text{Pr}_2$ group to the electron-deficient boron atom restricts the ring π -system to the NCN fragment, thus preventing the four-membered ring from being anti-aromatic. Organic synthetic methods were used to generate **4**,¹⁹ the synthesis of stable dianionic *bog* ligands, for example, $[\text{Pr}_2\text{NB}(\text{NDipp})_2]^{2-}$, has not been reported.



The report of carbene **4** stimulated our interest in the development of *bog* ligands to assess their broader utility

for the stabilization of reactive metal and non-metal centers. To this end we report herein (a) the synthesis and X-ray structural characterization of the new Dipp-substituted boranes ${}^i\text{Pr}_2\text{NB}(\text{NHDipp})_2$ (**5**), $\text{BrB}(\text{NHDipp})_2$ (**7b**), and $\text{B}(\text{NHDipp})_3$ (**8**), (b) a high yield synthesis and the X-ray structure of the first stable dilithio boraguanidinate $\{\text{Li}_2[{}^i\text{Pr}_2\text{NB}(\text{NDipp})_2]\}_2$ (**6**), and (c) a preliminary survey of the reactions of **6** with a variety of p-block and Group 12 element halides.

Experimental Section

Reagents and General Procedures. All reactions and the manipulation of moisture- and/or air-sensitive products were carried out under an atmosphere of argon using standard Schlenk line techniques or in an inert-atmosphere glovebox. Solvents were dried with appropriate drying agents, distilled before use, and stored over molecular sieves. Prior to use, all glassware was carefully dried. The reagents InCl (anhyd. 99.995%) and CdCl_2 (anhyd.) were purchased from Strem, TeI_4 (99%) and TiCl (99.99%) were purchased from Alfa Aesar, and all other chemicals were purchased from Aldrich Chemical Co. All chemicals were used as received, with the following exceptions: 2,6-diisopropylaniline (97%, Aldrich) was purified by distillation (at approximately 100 °C and 10^{-2} Torr) and anhydrous ZnCl_2 was prepared by heating $\text{ZnCl}_2 \cdot \text{H}_2\text{O}$ under vacuum (150 °C, 10^{-2} Torr, 18 h). The reagents $\text{LiN}(\text{H})\text{Dipp}$ and LiN^iPr_2 were prepared by the addition of ${}^i\text{BuLi}$ (2.5 M in hexane) in an equimolar amount to DippNH_2 or ${}^i\text{Pr}_2\text{NH}$, respectively, in *n*-hexanes, and purity was checked by ${}^1\text{H}$ NMR spectroscopy. Deuterated solvents were purchased from Cambridge Isotope Laboratories, dried over molecular sieves for at least one week, and degassed using the freeze-pump-thaw method.

Instrumentation. All NMR spectra were acquired at room temperature using a Bruker DRX 400 spectrometer. All chemical shifts are reported in parts per million (ppm) with higher frequency taken as positive. Chemical shifts for ${}^1\text{H}$ and ${}^{13}\text{C}\{{}^1\text{H}\}$ NMR spectra are reported with respect to tetramethylsilane and were calibrated based on the signal of the residual solvent peak. A solution of 1.0 M LiCl in D_2O was used as the external standard for ${}^7\text{Li}$ NMR spectra and ${}^{11}\text{B}\{{}^1\text{H}\}$ NMR chemical shifts are reported with respect to a solution of $\text{BF}_3 \cdot \text{OEt}_2$ in C_6D_6 . Elemental and mass spectrometry analyses (using a Waters GCT Premier spectrometer) were performed by the Analytical Services Laboratory of the Department of Chemistry, University of Calgary.

Crystal Structure Determinations. Single crystals of ${}^i\text{Pr}_2\text{NB}(\text{NHDipp})_2$ (**5**), $\{\text{Li}_2[{}^i\text{Pr}_2\text{NB}(\text{NDipp})_2]\}_2$ (**6**), $\text{BrB}(\text{NHDipp})_2$ (**7b**), and $\text{B}(\text{NHDipp})_3$ (**8**) suitable for X-ray analysis were covered with Paratone oil and mounted on a glass fiber in a stream of N_2 at 173 K on a Nonius KappaCCD diffractometer (Mo $\text{K}\alpha$ radiation, $\lambda = 0.71073 \text{ \AA}$) using the COLLECT (Nonius, B.V. 1998) software. The unit cell parameters were calculated and refined from the full data set. All crystal cell refinement and data reduction was carried out using the Nonius DENZO package. After data reduction, the data were corrected for absorption based on equivalent reflections using SCALEPACK (Nonius, B.V. 1998). The structures were solved by direct methods with the SHELXS-97²¹ program package and refinement was carried out on F^2 against all independent reflections by the full-matrix least-squares method by using the SHELXL-97 program.²² All non-hydrogen atoms were refined with anisotropic thermal parameters. The hydrogen atoms were calculated

- (13) Mohamed, A. A.; Mayer, A. P.; Abdou, H. E.; Irwin, M. D.; Pérez, L. M.; Fackler, J. P. *Inorg. Chem.* **2007**, *46*, 11165.
 (14) Ciobanu, O.; Emeljanenko, D.; Kaifer, E.; Mautz, J.; Himmel, H.-J. *Inorg. Chem.* **2008**, *47*, 4774.
 (15) For a recent review, see Fedorchuk, C.; Copey, M.; Chivers, T. *Coord. Chem. Rev.* **2007**, *251*, 897; the acronym *bam* is used as a generic representation of boraamidinate ligands.
 (16) Chivers, T.; Eisler, D. J.; Fedorchuk, C.; Schatte, G.; Tuononen, H. M.; Boeré, R. T. *Chem. Commun.* **2005**, 3930.
 (17) Konu, J.; Balakrishna, M. S.; Chivers, T.; Swaddle, T. W. *Inorg. Chem.* **2007**, *46*, 2627.
 (18) Braun, U.; Habereeder, T.; Nöth, H.; Piotrowski, H.; Warchhold, M. *Eur. J. Inorg. Chem.* **2002**, 1132.
 (19) Ishida, Y.; Donnadieu, B.; Bertrand, G. *Proc. Natl. Acad. Sci. U.S.A.* **2006**, *103*, 13585.
 (20) The acronym *bog* is suggested as a generic representation for boraguanidinate ligands.

- (21) Sheldrick, G.M. *SHELXS-97, Program for crystal structure determination*; University of Göttingen: Göttingen, Germany, 1997.
 (22) Sheldrick, G. M. *SHELXL-97, Program for refinement of crystal structures*; University of Göttingen: Göttingen, Germany, 1997.

geometrically and were riding on their respective atoms. Crystallographic data are summarized in Table 1. These data can be obtained free of charge from the Cambridge Crystallographic Data Centre via www.ccdc.cam.ac.uk/datarequest/cif.

Preparation of ${}^i\text{Pr}_2\text{NB}(\text{NHDipp})_2$ (5). A solution of ${}^i\text{Pr}_2\text{NB}(\text{Cl})_2$ (1.50 g, 8.20 mmol) in *n*-hexane (10 mL) was added to a stirred slurry of $\text{LiN}(\text{H})\text{Dipp}$ (3.05 g, 16.6 mmol) in *n*-hexane (25 mL) at 0 °C. The ice bath was removed after addition, and the reaction was allowed to warm to room temperature and stirred for 18 h. The reaction mixture was filtered and volatiles were removed in vacuo yielding **5** as a pale yellow solid (3.16 g, 6.80 mmol, 82%). Colorless, X-ray quality crystals were grown from two different *n*-hexane solutions, one exposed to air and the other air-protected. Anal. Calcd for $\text{C}_{30}\text{H}_{50}\text{BN}_3$: C, 77.73; H, 10.87; N, 9.06. Found: C, 77.35; H, 10.22; N, 8.96. ${}^1\text{H}$ NMR (C_6D_6 , 25 °C): δ 7.13 (m, 6 H, Dipp), 3.68 (sept, 4 H, $-\text{CH}(\text{CH}_3)_2$ of Dipp groups, ${}^3J_{\text{H-H}} = 6.8$ Hz), 3.30 (2 H, br s, $-\text{NH}$), 3.24 (sept, 2 H, $-\text{CH}(\text{CH}_3)_2$ of $-\text{N}^i\text{Pr}_2$ groups, ${}^3J_{\text{H-H}} = 6.8$ Hz), 1.28 (d, 12 H, $-\text{CH}(\text{CH}_3)_2$ of Dipp groups, ${}^3J_{\text{H-H}} = 6.8$ Hz), 1.18 (d, 12 H, $-\text{CH}(\text{CH}_3)_2$ of Dipp groups, ${}^3J_{\text{H-H}} = 6.8$ Hz), 1.11 (d, 12 H, $\text{CH}(\text{CH}_3)_2$ of $-\text{N}^i\text{Pr}_2$ groups, ${}^3J_{\text{H-H}} = 6.8$ Hz). ${}^{11}\text{B}$ NMR (C_6D_6 , 25 °C): δ 23.4. ${}^{13}\text{C}$ NMR (C_6D_6 , 25 °C): δ 146.5 (Dipp), 139.8 (Dipp), 126.0 (Dipp), 123.6 (Dipp), 45.3 ($-\text{CH}(\text{CH}_3)_2$ of $-\text{N}^i\text{Pr}_2$ groups), 29.1 ($-\text{CH}(\text{CH}_3)_2$ of Dipp groups), 24.5 ($-\text{CH}(\text{CH}_3)_2$ of Dipp groups), 24.3 ($-\text{CH}(\text{CH}_3)_2$ of $-\text{N}^i\text{Pr}_2$ groups), 24.0 ($-\text{CH}(\text{CH}_3)_2$ of Dipp groups). Mp: 123–126 °C.

Preparation of $\text{Li}_2[{}^i\text{Pr}_2\text{NB}(\text{NDipp})_2]$ (6). A 2.5 M solution of ${}^n\text{BuLi}$ in hexanes (2.0 mL, 5.0 mmol) was added to a solution of ${}^i\text{Pr}_2\text{NB}(\text{NHDipp})_2$ (1.16 g, 2.49 mmol) in *n*-hexane (20 mL) at -30 °C. The reaction mixture was allowed to warm to room temperature and stirred for 18 h. Volatiles were removed in vacuo to give **6** as a pale yellow solid (1.004 g, 2.10 mmol, 85%). Colorless, X-ray quality crystals were grown from an *n*-hexane/toluene mixture. Anal. Calcd for $\text{C}_{66}\text{H}_{110}\text{N}_6\text{B}_2\text{Li}_4$ (dimer + co-crystallized hexane molecule): C, 76.44; H, 10.69; N, 8.10. Found: C, 76.12; H, 10.93; N, 7.92. ${}^1\text{H}$ NMR (THF-d_8 , 25 °C): δ 6.77 (m, 4 H, Dipp), 6.23 (m, 2 H, Dipp), 3.84 (br sept, 4 H, $-\text{CH}(\text{CH}_3)_2$ of Dipp groups), 3.65 (br sept, 2 H, $\text{CH}(\text{CH}_3)_2$ of $-\text{N}^i\text{Pr}_2$ groups), 1.20 (d, 12 H, $-\text{CH}(\text{CH}_3)_2$ of Dipp groups, ${}^3J_{\text{H-H}} = 6.8$ Hz), 1.07 (d, 12 H, $-\text{CH}(\text{CH}_3)_2$ of Dipp groups, ${}^3J_{\text{H-H}} = 6.8$ Hz), 0.92 (d, 12 H, $\text{CH}(\text{CH}_3)_2$ of $-\text{N}^i\text{Pr}_2$ groups, ${}^3J_{\text{H-H}} = 6.9$ Hz). ${}^{11}\text{B}$ NMR (THF-d_8 , 25 °C): δ 22.8. ${}^7\text{Li}$ NMR (THF-d_8): δ 0.87. ${}^{13}\text{C}$ NMR (THF-d_8 , 25 °C): δ 157.9 (Dipp), 139.2 (Dipp), 122.7 (Dipp), 46.9 ($-\text{CH}(\text{CH}_3)_2$ of $-\text{N}^i\text{Pr}_2$ groups), 27.9 ($-\text{CH}(\text{CH}_3)_2$ of Dipp groups), 26.5 ($-\text{CH}(\text{CH}_3)_2$ of Dipp groups), 25.8 ($-\text{CH}(\text{CH}_3)_2$ of $-\text{N}^i\text{Pr}_2$ groups), 24.9 ($-\text{CH}(\text{CH}_3)_2$ of Dipp groups).

Preparation of $\text{ClB}(\text{NHDipp})_2$ (7a). A solution of DippNH_2 (4.26 g, 24.0 mmol) in *n*-hexane (40 mL) was added to a solution of BCl_3 in *n*-hexane (6 mL, 6 mmol) at -80 °C. A white precipitate formed shortly after the addition. The reaction mixture was warmed to room temperature and stirred for 18 h. It was then filtered and volatiles were removed in vacuo to give **7a** as a colorless solid (1.71 g, 72%). Anal. Calcd for $\text{C}_{24}\text{H}_{36}\text{BN}_2\text{Cl}$: C, 72.28; H, 9.10; N, 7.02. Found: C, 73.08; H, 9.45; N, 7.05. ${}^1\text{H}$ NMR (C_6D_6 , 25 °C): δ 7.17–7.06 (m, 6 H, Dipp), 4.14 (br, 1 H), 3.72 (br, 1 H), 3.57 (br s, 2 H), 3.38 (br, 2 H), 1.20 (overlapping doublets, 24 H, $\text{CH}(\text{CH}_3)_2$ of Dipp groups). ${}^{11}\text{B}$ NMR (C_6D_6 , 25 °C): δ 26.4. ${}^{13}\text{C}$ NMR (C_6D_6 , 25 °C): δ 147 (Dipp), 137 (Dipp), 124 (Dipp), 28.9 ($-\text{CH}(\text{CH}_3)_2$ of Dipp groups), 24.3 ($-\text{CH}(\text{CH}_3)_2$ of Dipp groups). HRMS: Calculated m/z for $[\text{C}_{24}\text{H}_{36}\text{N}_2\text{BCl}]$: 398.2660. Found: 398.2680. MP: 67–69 °C.

Preparation of $\text{BrB}(\text{NHDipp})_2$ (7b). The bromo derivative **7b** was obtained as a colorless solid (0.87 g, 4.2 mmol, 47%) from DippNH_2 (2.85 g, 16.1 mmol) in *n*-hexane (15 mL) and BBr_3 (1.04

g, 4.15 mmol) in *n*-hexane (15 mL) at -80 °C by using a procedure similar to that described for **7a**. Anal. Calcd for $\text{C}_{24}\text{H}_{36}\text{BN}_2\text{Br}$: C, 65.03; H, 8.19; N, 6.32. Found: C, 64.64; H, 8.34; N, 6.34. ${}^1\text{H}$ NMR (C_6D_6 , 25 °C): δ 7.19–7.10 (m, 6 H, Dipp), 4.37 (br, 1 H), 3.94 (br, 1 H), 3.60 (br s, 2 H), 3.41 (br, 2 H), 1.19 (overlapping doublets, 24 H, $\text{CH}(\text{CH}_3)_2$). ${}^{11}\text{B}$ NMR (C_6D_6 , 25 °C): δ 25.7. ${}^{13}\text{C}$ NMR (C_6D_6 , 25 °C): δ 147 (Dipp), 136.8 (Dipp), 135.9 (Dipp), 123.9 (Dipp), 29.0 ($\text{CH}(\text{CH}_3)_2$ of Dipp groups), 24.3 ($-\text{CH}(\text{CH}_3)_2$ of Dipp groups). LRMS: Calculated m/z for $[\text{C}_{24}\text{H}_{36}\text{N}_2\text{BBr}]$: 442.2. Found: 442.2. MP: 109–112 °C.

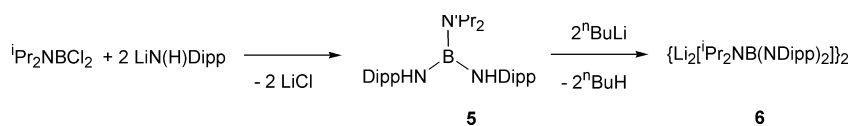
Preparation of $\text{B}(\text{NHDipp})_3$ (8). A solution of DippNH_2 (6.38 g, 36 mmol) in *n*-hexane (40 mL) was added to a stirred solution of BCl_3 in *n*-hexane (6.0 mL, 6.0 mmol) at -80 °C. A white precipitate began to form upon addition. The reaction mixture was allowed to warm to room temperature and stirred for 18 h. After filtration, volatiles were removed in vacuo yielding **8** as a white sticky solid (3.0 g, 5.6 mmol, 93%). Colorless, X-ray quality crystals were grown from an air-protected *n*-hexane solution. Anal. Calcd for $\text{C}_{36}\text{H}_{54}\text{BN}_3$: C, 80.12; H, 10.09; N, 7.79. Found: C, 79.62; H, 10.12; N, 7.72. ${}^1\text{H}$ NMR (C_6D_6 , 25 °C): δ 7.13 (m, Dipp), 7.02 (m, Dipp), 3.73 (sept, 6 H, $\text{CH}(\text{CH}_3)_2$ of Dipp groups, ${}^3J_{\text{H-H}} = 6.9$ Hz), 3.26 (s, 3 H, $-\text{NH}$), 1.24, 1.19 (overlapping d, 36 H, $\text{CH}(\text{CH}_3)_2$ of Dipp groups). ${}^{11}\text{B}$ NMR (C_6D_6 , 25 °C): δ 22.6. ${}^{13}\text{C}$ NMR (C_6D_6 , 25 °C): δ 147.1 (Dipp), 137.4 (Dipp), 126.6 (Dipp), 123.9 (Dipp), 28.9 ($-\text{CH}(\text{CH}_3)_2$ of Dipp groups), 24.1 ($-\text{CH}(\text{CH}_3)_2$ of Dipp groups). HRMS: Calculated m/z for $[\text{C}_{36}\text{H}_{54}\text{BN}_3]$: 539.4411. Found: 539.4416. MP: 167–170 °C.

Alternative Synthesis of $\text{Li}_2[{}^i\text{Pr}_2\text{NB}(\text{NDipp})_2]$ (6). A solution of $\text{B}(\text{NHDipp})_3$ (0.334 g, 0.62 mmol) in *n*-hexane (12 mL) was added to a slurry of LDA (0.20 g, 1.87 mmol) in *n*-hexane (12 mL) at -40 °C. The reaction was maintained at this temperature for 45 min then allowed to warm to room temperature and stirred for 18 h. The mixture was filtered and volatiles were removed in vacuo to give a yellow solid (0.285 g). The ${}^1\text{H}$ NMR spectrum showed the presence of $\text{Li}_2[{}^i\text{Pr}_2\text{NB}(\text{NDipp})_2]$ (**6**) as the major product, together with a minor unidentified impurity.

Reaction of $\text{Li}_2[\text{PhB}(\text{NDipp})_2]$ with InCl . A solution of $\text{Li}_2[\text{PhB}(\text{NDipp})_2]^{23}$ (0.20 g, 0.45 mmol) in Et_2O was added to a slurry of InCl (0.069 g, 0.46 mmol) in Et_2O at -70 °C. The reaction mixture immediately turned dark brown with formation of a precipitate. The mixture was allowed to warm to room temperature and stirred for 4 h. After filtration to remove indium metal and LiCl and evaporation of volatiles in vacuo, an orange-yellow solid was isolated and the major product was determined to be the spirocyclic indium(III) complex $\text{LiIn}[\text{PhB}(\text{NDipp})_2]_2$.¹⁸ ${}^1\text{H}$ NMR (C_6D_6 , 25 °C): δ 7.29–6.73 (m, 22 H, aryl of Dipp and Ph), 4.47 (sept, 4 H, $-\text{CH}(\text{CH}_3)_2$, ${}^3J_{\text{H-H}} = 7$ Hz), 3.81 (sept, 4 H, $-\text{CH}(\text{CH}_3)_2$, ${}^3J_{\text{H-H}} = 7$ Hz), 2.93 (q, Et_2O), 1.73 (d, 12 H, $-\text{CH}(\text{CH}_3)_2$, ${}^3J_{\text{H-H}} = 7$ Hz), 1.64 (d, 12 H, $-\text{CH}(\text{CH}_3)_2$, ${}^3J_{\text{H-H}} = 7$ Hz), 0.82 (d, 12 H, $-\text{CH}(\text{CH}_3)_2$, ${}^3J_{\text{H-H}} = 7$ Hz), 0.77 (t, Et_2O), 0.65 (d, 12 H, $-\text{CH}(\text{CH}_3)_2$, ${}^3J_{\text{H-H}} = 7$ Hz). ${}^{11}\text{B}$ NMR (C_6D_6 , 25 °C): δ 30 ppm (br, s).

Synthesis of $\{\text{Ge}[{}^i\text{Pr}_2\text{NB}(\text{NDipp})_2]\}_2 \cdot \text{dioxane}$ (10). A solution of **6** (0.012 g, 0.025 mmol) in THF-d_8 was added to solid $\text{GeCl}_2 \cdot (\text{C}_4\text{H}_8\text{O}_2)$ (0.006 g, 0.026 mmol) in an NMR tube. As the $\text{GeCl}_2 \cdot (\text{C}_4\text{H}_8\text{O}_2)$ dissolved and reacted, the color of the solution changed from pale yellow to golden orange. NMR data were collected on this solution. ${}^1\text{H}$ NMR (THF-d_8 , 25 °C): δ 7.04 (d, 4 H, Dipp), 6.87 (t, 2 H, Dipp), 3.80 (sept, 4 H, $\text{CH}(\text{CH}_3)_2$ of Dipp groups, ${}^3J_{\text{H-H}} = 6.9$ Hz), 3.57 (s, 4H, dioxane), 3.26 (sept, 2 H, $\text{CH}(\text{CH}_3)_2$ of N^iPr_2 groups, ${}^3J_{\text{H-H}} = 6.9$ Hz), 1.30 (d, 12 H,

Scheme 1



CH(CH₃)₂ of Dipp groups, ³J_{H-H} = 6.9 Hz), 1.16, (d, 12 H, CH(CH₃)₂ of Dipp groups, ³J_{H-H} = 6.9 Hz), 0.86 (d, 12 H, CH(CH₃)₂ of NⁱPr₂ groups, ³J_{H-H} = 6.9 Hz). ¹¹B NMR (THF-d₈, 25 °C): δ 28.04. ¹³C NMR (THF-d₈, 25 °C): δ 145.2, 123.4, 123.2, 68.0, 45.7, 28.8, 28.0, 25.0, 23.4.

Synthesis of Mg[ⁱPr₂NB(NDipp)₂] (11). A mixture of **6** (0.189 g, 0.40 mmol) and MgCl₂ (0.038 g, 0.40 mmol) was dissolved in THF (15 mL) and heated at 60 °C for 4 h. Volatiles were removed in vacuo to give **11** as an orange solid (0.085 g, 44%). ¹H NMR (THF-d₈, 25 °C): δ 6.67 (d, 4 H, Dipp), 6.25 (t, 2 H, Dipp), 4.15 (sept, 4 H, CH(CH₃)₂ of Dipp groups, ³J_{H-H} = 6.74 Hz), 3.43 (sept, 2 H, -CH(CH₃)₂ of -NⁱPr₂ groups, ³J_{H-H} = 6.72 Hz), 1.18 (d, 12 H, ³J_{H-H} = 6.74 Hz), 1.09 (d, 12 H, ³J_{H-H} = 6.72 Hz), 0.76 (d, 12 H, ³J_{H-H} = 6.88 Hz). ¹¹B NMR (THF-d₈, 25 °C): δ 23.2. ¹³C NMR (THF-d₈, 25 °C): δ 157.5, 141.7, 122.5, 115.0, 47.1, 27.9, 26.5, 24.8.

Synthesis of Zn[ⁱPr₂NB(NDipp)₂] (12). A solution of **6** (0.372 g, 0.78 mmol) in THF (10 mL) was added to solid ZnCl₂ (0.107 g, 0.79 mmol) and stirred for 30 min. Volatiles were removed in vacuo and the product was extracted with Et₂O (20 mL) and filtered. Removal of volatiles in vacuo gave **12** as pale yellow solid (0.335 g, 0.50 mmol, 63%). ¹H NMR (THF-d₈, 25 °C): δ 6.74 (d, 4 H, Dipp), 6.42 (t, 2 H, Dipp), 4.15 (sept, 4 H, CH(CH₃)₂ of Dipp groups, ³J_{H-H} = 6.8 Hz), 3.30 (sept, 2 H, CH(CH₃)₂ of NⁱPr₂ groups, ³J_{H-H} = 6.87 Hz), 1.21 (d, 12 H, CH(CH₃)₂ of Dipp groups, ³J_{H-H} = 6.8 Hz), 1.13, (d, 12 H, CH(CH₃)₂ of Dipp groups, ³J_{H-H} = 6.8 Hz), 0.76 (d, 12 H, CH(CH₃)₂ of NⁱPr₂ groups, ³J_{H-H} = 6.8 Hz). ¹¹B NMR (THF-d₈, 25 °C): δ 25.2. ¹³C NMR (THF-d₈, 25 °C): δ 154.2, 143.1, 121.9, 117.0, 46.7, 28.2, 25.0, 23.3.

Results and Discussion

Synthesis and Characterization of ⁱPr₂NB(NHDipp)₂ (5) and {Li₂[ⁱPr₂NB(NDipp)₂]}₂ (6). The reaction of ⁱPr₂NBCl₂ with 2 equiv of lithium 2,6-diisopropylphenyl amide, LiN(H)(Dipp), in *n*-hexane produces the neutral ligand ⁱPr₂NB(NHDipp)₂ (**5**) in >80% yield (Scheme 1).

Colorless crystals of **5** suitable for X-ray diffraction were grown from a *n*-hexane solution in air, and the molecular structure is shown in Figure 1. Selected bond lengths and angles are presented in Table 3. The geometry at boron is slightly distorted from trigonal with bond angles in the range 116.0–123.3°; however, the sum of these angles is 360°. The nitrogen atoms also display distorted trigonal geometries, having bond angles ranging from about 114 to 131°, though the sum of the angles about each nitrogen is 360°. There is no significant difference in the B–NⁱPr₂ and B–N(H)Dipp bond lengths, which are intermediate between single and double bond values, as expected for N(2p)→B(2p) π-bonding.

Deprotonation of **5** with 2 equiv of ⁿbutyllithium in hexanes (Scheme 1) gives the dianionic ligand as the dilithio derivative {Li₂[ⁱPr₂NB(NDipp)₂]}₂ (**6**) in isolated yields of >90%. This new boroguanidinate reagent is soluble in hexane, and X-ray quality crystals were grown from this

solvent. The molecular structure of **6** reveals the formation of a dimeric cluster in the solid state with a co-crystallized solvent molecule (Figure 2, hexane molecule omitted for clarity).

The sum of the bond angles about boron is 360°; however, the geometry is distorted from trigonal, with the N(1)–B(1)–N(2) angle being about 7° smaller than the corresponding bond angle in the acyclic neutral ligand **5** (109° vs 116°), presumably as a result of the constraints imposed by the cluster structure. The dimeric nature of **6** parallels our previous observations for the unsolvated dilithio *bam*'s: {Li₂[RB(NⁱBu)₂]}₂ (R = Me,²⁴ ⁿBu,²⁴ Ph,²⁵ and ^tBu²⁵). In addition to the dimer {Li₂[MeB(NⁱBu)₂]}₂, a trimeric structure is also observed for the *B*-methyl derivative {Li₂[MeB(NⁱBu)₂]}₃.²⁴ A comparison of relevant bond lengths and bond angles in **6** with those of selected dilithio *bam*'s is found in Table 2.

To fully appreciate any structural effects imposed by the diisopropylamino group in **6**, a comparison with an analogous *N*-Dipp-substituted *bam* complex {Li₂[RB(NDipp)₂]}₂ is desirable. However, the only known example is the trisolvated complex (*μ*-THF)[Li(THF)₂][PhB(NDipp)₂], which exists as a monomer in the solid state owing to solvation of the Li⁺ cations.²³ In contrast to {Li[PhB(NDipp)₂]}₂, the boroguanidinate **6** is hexane-soluble so crystals can be grown without exposure to a coordinating solvent; dimer formation increases the coordination number of the lithium cation through an additional nitrogen contact, as previously observed in unsolvated dilithio *bam*'s.^{24,25} The N(1)–B(1)–N(2) bond angle in **6** is slightly narrower than that in the monomer (*μ*-THF)[Li(THF)₂][PhB(NDipp)₂] (109.1° versus 111.4°), likely as a result of the constrained geometry imposed by dimer formation. The B–N bond lengths in **6** are also slightly elongated with respect to those in (*μ*-THF)[Li(THF)₂][PhB(NDipp)₂], as a consequence of the additional amino group contributing electron density to the boron center.

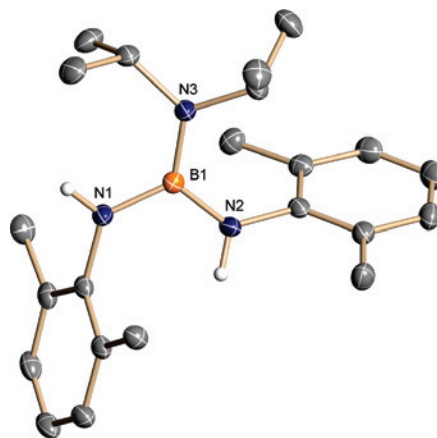


Figure 1. Molecular structure of **5**. Hydrogen atoms are omitted and only the α -carbon atoms of Dipp groups are shown for clarity.

Table 1. Crystallographic Data for **5**, **6**, **7b**, and **8**^a

	5	6	7b	8
empirical formula	C ₃₀ H ₅₀ B N ₃	C ₃₃ H ₅₅ BLi ₂ N ₃	C ₂₄ H ₃₆ BBrN ₂	C ₃₆ H ₅₄ BN ₃
fw	463.54	518.49	443.27	539.63
cryst. system	orthorhombic	orthorhombic	monoclinic	monoclinic
space group	<i>Pbca</i>	<i>Pbcn</i>	<i>P2(1)/n</i>	<i>P2(1)/n</i>
<i>a</i> , Å	18.7744(4)	14.103(3)	19.626(4)	10.744(2)
<i>b</i> , Å	15.687(3)	21.061(4)	6.426(1)	28.035(6)
<i>c</i> , Å	20.218(4)	21.701(4)	20.311(4)	11.875(2)
α, deg.	90.00	90.00	90.00	90.00
β, deg.	90.00	90.00	103.98(3)	112.08(3)
γ, deg.	90.00	90.00	90.00	90.00
<i>V</i> , Å ³	5954(2)	6446(2)	2486(1)	3314(1)
<i>Z</i>	8	8	2	4
<i>T</i> , °C	−100	−100	−100	−100
ρ _{calcd} , g/cm ³	1.034	1.069	1.184	1.081
μ(Mo Kα), mm ^{−1}	0.059	0.060	1.665	0.062
crystal size, mm ³	0.40 × 0.36 × 0.28	0.40 × 0.16 × 0.08	0.08 × 0.08 × 0.04	0.28 × 0.28 × 0.16
<i>F</i> (000)	2048	2280	936	1184
Θ range, deg	3.38–25.03	2.56–25.03	3.35–25.03	2.99–25.03
reflns collected	87203	34800	46407	42938
unique reflns	5242	5663	4379	5830
<i>R</i> _{int}	0.0234	0.0502	0.1371	0.0393
<i>R</i> ₁ [<i>I</i> > 2σ(<i>I</i>)] ^b	0.0468	0.0627	0.0643	0.0583
<i>wR</i> ₂ (all data) ^c	0.1238	0.1749	0.1566	0.1507
GOF on <i>F</i> ²	1.033	1.030	1.039	1.032
completeness	0.996	0.994	0.995	0.996

^a λ(Mo Kα) = 0.71073 Å. ^b *R*₁ = Σ||*F*_o| − |*F*_c||/Σ|*F*_o|. ^c *wR*₂ = [Σ*w*(*F*_o² − *F*_c²)/Σ*wF*_o⁴]^{1/2}.

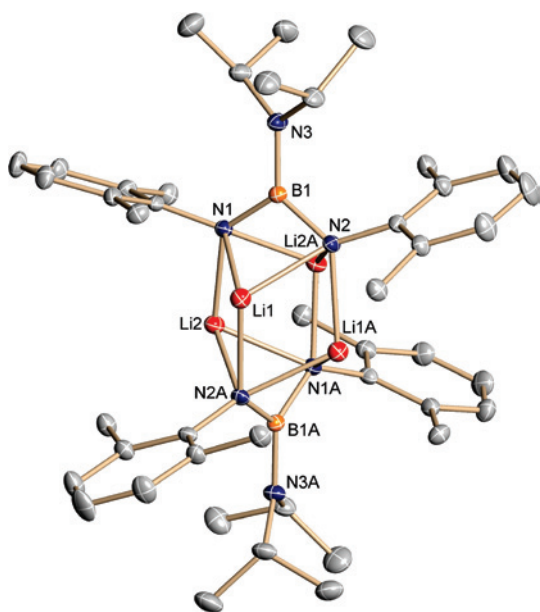


Figure 2. Molecular structure of **6**. Hydrogen atoms are omitted and only the α-carbon atoms of Dipp groups are shown for clarity. Symmetry elements used to generate equivalent atoms: #1, $-x + 1, y, -z + 1/2$; #2, $-x, -y, -z + 1$.

The B–N distances in **6** are not significantly different from those in the dimeric *B*-alkyl *bam*'s {Li₂[RB(NⁿBu)₂]} (R = ⁿBu, ^tBu), but they are slightly elongated when compared to those in the *B*-phenyl derivative {Li₂[PhB(NⁿBu)₂]}₂; this is likely a result of the electron-donating nature of the dialkylamino or alkyl substituents on boron compared to the electron-withdrawing phenyl group. The nitrogen–lithium distances in **6** fall within the expected range for three-coordinate nitrogen centers.

The direct metalation reaction (alkane elimination) is successful for the preparation of the magnesium *bam* complex Mg(OEt)₂[PhB(NDipp)₂] from PhB(NHDipp)₂ and

Table 2. Bond Lengths (Å) and Bond Angles (deg) for **6** and Dimeric Dilithioboraamidates

	6	{Li ₂ [ⁿ BuB(N ⁿ Bu) ₂]} ₂ ^a	{Li ₂ [PhB(N ⁿ Bu) ₂]} ₂ ^b	{Li ₂ [^t BuB(N ⁿ Bu) ₂]} ₂ ^b
B1–N1	1.471(3)	1.455(4)	1.448(3)	1.476(4)
B1–N2	1.470(3)	1.464(4)	1.449(3)	1.479(4)
Li1–N1	2.055(5)	2.032(5)	2.077(4)	1.980(4)
Li1–N2	2.121(5)	2.039(6)	2.052(4)	2.154(5)
Li1–N2A	2.144(5)	2.027(5)	2.017(4)	2.125(4)
Li2–N1	2.063(5)	2.032(5)	2.027(4)	2.154(5)
Li2–N2A	2.063(5)	2.022(6)	2.022(4)	1.976(4)
Li2–N1A	2.145(5)	2.091(5)	2.074(4)	1.976(4)
N1–B1–N2	109.1(2)	108.2(2)	109.5(2)	105.2(2)
N3–B1–N2	126.1(2)	N/A	N/A	N/A
N3–B1–N1	124.8(2)	N/A	N/A	N/A

^a Ref 24. ^b Ref 25.

Table 3. Selected Bond Lengths (Å) and Bond Angles (deg) for **5**, **7b**, and **8**

	5	7b	8
B1–N1	1.438(2)	1.383(7)	1.423(3)
B1–N2	1.437(2)	1.402(7)	1.427(3)
B1–Br1		1.951(6)	
B1–N3	1.429(2)		1.426(3)
N3–B1–N1	120.66(13)		120.61(19)
N3–B1–N2	123.32(14)		119.04(18)
N1–B1–N2	116.01(13)	123.5(5)	120.35(18)
N1–B1–Br1		119.2(4)	
N2–B1–Br1		117.2(4)	

an excess of ⁿsBu₂Mg.²⁶ By contrast, the neutral *bog* ligand **5** was recovered unchanged from attempted reactions with dibutyl magnesium, dimethyl zinc, or trimethyl aluminum at various temperatures in either coordinating or non-coordinating solvents.

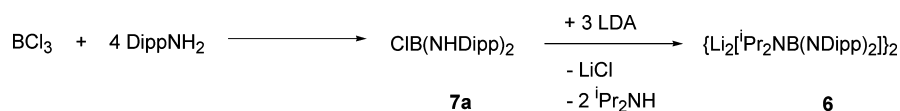
Oxidation with I₂ - Radical Formation. Exposure of dilithio *bam*'s to air produces persistent bright pink solutions,

(24) Brask, J. K.; Chivers, T.; Schatte, G. *Chem. Commun.* **2000**, 1805.

(25) Chivers, T.; Fedorchuk, C.; Schatte, G.; Brask, J. K. *Can. J. Chem.* **2002**, *80*, 821.

(26) Chivers, T.; Eisler, D. J.; Fedorchuk, C.; Schatte, G.; Tuononen, H. M.; Boeré, R. T. *Inorg. Chem.* **2006**, *45*, 2119.

Scheme 2



indicative of radical formation.²⁵ The one-electron oxidation of $\{\text{[PhB(N}^t\text{Bu)}_2\text{][Li}_2]\}_2$ with 0.5 equiv of I_2 generates the thermally unstable, monomeric neutral radical, $\{\text{[PhB}(\mu\text{-N}^t\text{Bu)}_2\text{Li(OEt)}_x\}^{\cdot}$, in which the radical anion $\text{[PhB(N}^t\text{Bu)}_2\text{]}^{\cdot-}$ is N,N' -chelated to a solvated Li^+ cation.²⁶ This radical was characterized by a combination of low-temperature electron paramagnetic resonance (EPR) spectroscopy and density-functional theory (DFT) calculations. To compare the behavior of boraguanidates upon oxidation with that of boraamidates, the reaction of **6** with 0.5 equiv of I_2 was carried out at -100°C . Upon addition of the orange-red I_2 solution a transient violet color was observed, which disappeared rapidly to give a golden yellow solution and an EPR spectrum could not be obtained. Subsequently, a pale cream solid was isolated and was found to contain the diprotonated derivative $\text{Pr}_2\text{NB(NHDipp)}_2$ (**5**) as the major product by ^1H NMR spectroscopy. These qualitative observations indicate that the neutral *bog* radical $\{\text{[Pr}_2\text{B}(\mu\text{-NDipp)}_2\text{Li(OEt)}_x\}^{\cdot}$ has lower thermal stability than the *bam* radical $\{\text{[PhB}(\mu\text{-N}^t\text{Bu)}_2\text{Li(OEt)}_x\}^{\cdot}$.²⁶

Alternative Syntheses of 6: Synthesis and X-ray Structures of BrB(NHDipp)₂ and B(NHDipp)₃. An alternative synthetic approach to **6** involves the reaction of BCl_3 with 4 equiv of DippNH_2 to form ClB(NHDipp)_2 (**7a**), followed by the addition of 3 equiv of lithium diisopropyl amide LiN^iPr_2 (LDA) (Scheme 2). The reagent LDA serves the dual purpose of installing the diisopropylamino group as a substituent on boron and deprotonating both -NHDipp groups in a one-pot process.

The chloroborane, Cl(BNHDipp)_2 (**7a**), was produced as a colorless solid in 72% yield and characterized by elemental analysis, high resolution mass spectrometry and multinuclear (^1H , ^{11}B , and ^{13}C) NMR spectroscopy; however, crystals isolated from a concentrated *n*-hexane solution were fibrous needles not suitable for X-ray diffraction. Consequently, the bromine derivative, BrB(NHDipp)_2 (**7b**), was prepared as a colorless solid in 47% yield by the analogous reaction of BBr_3 and 4 equiv of DippNH_2 . Spectroscopic data of **7b** revealed the expected small upfield shift of the ^{11}B resonance (25.7 vs 26.4 ppm), and the ^1H NMR data were comparable with that of **7a**. Compound **7b** was also characterized by elemental analysis and mass spectrometry and was found to have a higher melting range than its chlorine counterpart ($109\text{--}112^\circ$ vs $67\text{--}69^\circ$). Crystals suitable for X-ray diffraction formed from an *n*-hexane solution, and the molecular structure is shown in Figure 3.

The B-N(H)Dipp bond distances in **7b** are slightly shorter than those found in **5** (Table 3), a result of the replacement of one of the amino groups by the more weakly π -bonding bromine atom. The geometry about boron is distorted from trigonal planar although the sum of the angles is 360° . The B-Br distance is, within experimental error, the same as found for a bromo-diazaborole,²⁷ which provides a compa-

table three-coordinate boron environment containing a bromine and two nitrogen substituents. To minimize steric interactions, the Dipp groups are oriented perpendicular to the N-B-N plane, with dihedral angles of 90.0° and 91.5° for $\text{B(1)-N(1)-C(1)-C(2)}$ and $\text{B(1)-N(2)-C(13)-C(14)}$, respectively.

The addition of a solution of chloroborane **7a** in toluene to 3 equiv of LDA at 0°C produced a pale yellow solid, which was shown by the ^1H NMR spectrum to be primarily the dilithio *bog* **6**, together with a minor unidentified impurity. Although this reaction represents an alternative synthesis of **6**, the method shown in Scheme 1 is preferable. However, the novel haloboranes **7a** and **7b** are potentially useful reagents for the preparation of other *bam* or *bog* ligands via reactions with alkyl-, aryl-, or amido-lithium reagents.

We have previously shown that treatment of the tris(alkylamino)boranes $(^t\text{BuNH})_3\text{B}$ with 3 equiv of an organolithium reagent RLi ($\text{R} = \text{Me}$, ^tBu) produces the dilithio *bam*'s $\{\text{Li}_2\{\text{RB(N}^t\text{Bu)}_2\}\}_n$ ($\text{R} = \text{Me}$, $n = 2, 3$; $\text{R} = ^t\text{Bu}$, $n = 2$) via a process that involves the concomitant nucleophilic displacement of one $^t\text{BuNH}$ by an R group on boron and the deprotonation of the other two RNH groups.²⁴ Thus, the reaction of $(\text{DippNH})_3\text{B}$ (**8**) with 3 equiv of LDA represents another possible route to **6**. With this objective in mind the tris(arylamino)borane **8** was obtained in 93% yield as colorless crystals from the reaction of BCl_3 and 6 equiv of DippNH_2 in *n*-hexane. The borane **8** was characterized by elemental analysis, high resolution mass spectrometry, multinuclear (^1H , ^{11}B , and ^{13}C) NMR spectroscopy, and a single crystal X-ray structural determination. The ^{11}B NMR chemical shift of **8** is about 4 ppm upfield from that of the chloroborane **7a**.

The X-ray analysis of **8** confirmed the expected trigonal geometry (Figure 4). A comparison of selected bond lengths and bond angles for **5**, **7b**, and **8** is found in Table 3. The B-N(H)Dipp bond distances in **8** are similar to those found

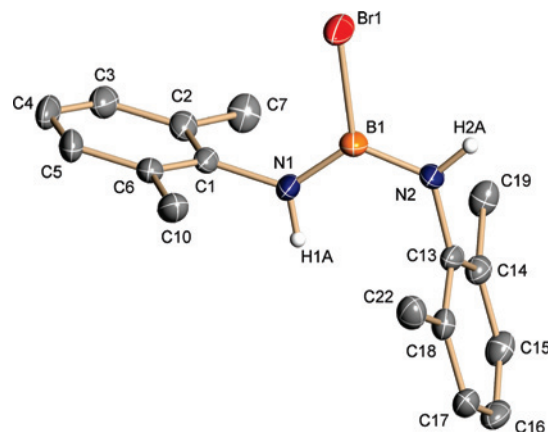


Figure 3. Molecular structure of **7b**. Hydrogen atoms are omitted, and only the α -carbon atoms of Dipp groups are shown for clarity.

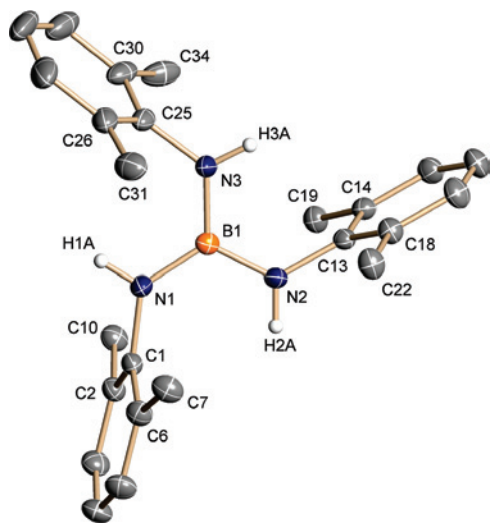


Figure 4. Molecular structure of $B(NHDipp)_3$, **8**. Hydrogen atoms are omitted, and only the α -carbon atoms of Dipp groups are shown for clarity.

in **5** (vide supra), and the geometry about boron is almost perfectly trigonal planar with the sum of the angles being 360° . To minimize steric interactions, two of the three Dipp groups are oriented perpendicular to the N–B–N plane, with dihedral angles of 93.0 and 88.6° for B(1)–N(1)–C(1)–C(2) and B(1)–N(2)–C(13)–C(14), respectively, while the third Dipp group is twisted slightly further, with a B(1)–N(3)–C(25)–C(30) torsion angle of 102.1° .

The addition of 3 equiv of LDA to **8** produced **6** (1H NMR), together with the same impurity previously observed in the synthesis depicted in Scheme 2. Although **6** can be produced by these two alternative methods, the synthesis using the commercially available $^iPr_2NB(Cl)_2$ (Scheme 1) is the most efficient route to the new *bog* ligand.

Reactions of 6 with p-Block and Group 12 Element Halides. To compare the applications of the new Li_2bog **6** as a metathetical reagent with the well-established uses of dilithio *bam*'s,¹⁵ the reactions of **6** with selected p-block and group 12 element halides were investigated. Although **6** was effective in metathesis in some cases, it was also found to be a strong reducing agent toward many p-block element halides or to give products that disproportionate with deposition of the metal.

(a) Reduction. The reactions of **6** with a variety of p-block or group 12 metal halides, for example, $SnCl_2$, $PbCl_2$, $TeBr_4$, TeI_4 , $CdCl_2$, and $TlCl$, resulted in the instantaneous deposition of the respective metal upon mixing of the reagents either at room temperature or below. In most cases, after removal of the metal via filtration, the isolated solid from these reactions contained two or more major products by 1H NMR spectroscopy.

The behavior of **6** in the reactions with tin(II) and lead(II) dichlorides differs from that of dilithio *bam*'s, which produce stable dimeric complexes $M(bam)_2$ ($M = Sn, Pb$) via metathesis.^{28,29} In fact, the lead(II) dimer $\{Pb[PhB(N^iBu)_2]\}_2$ was initially prepared by the reduction of $PbCl_4$ with $Li_2[PhB(N^iBu)_2]$, although it is more conveniently prepared directly from $PbCl_2$.²⁹ The immediate precipitation of Pb metal in the reaction of **6** with $PbCl_2$ demonstrates the strong

reducing power of the *bog* ligand, which is attributed to its increased electron-richness when compared to the dilithio *bam*'s.

The reduction of Tl(I) to Tl in the reaction of **6** and 2 equiv of $TlCl$ is not unprecedented, since Manke and Nocera observed the formation of thallium metal in the reaction of $Li_2[PhB(NR)_2]$ ($R = ^iPr, ^tBu$) with $TlCl$.³⁰ However, these authors were able to isolate the polymeric thallium(I) *bam* complexes $\{Tl_2[PhB(NR)_2]\}_\infty$ in moderate yields from these reactions. By contrast, the major product of the reaction of **6** and $TlCl$ was identified as $^iPr_2NB(NHDipp)_2$ (**5**) by 1H NMR spectroscopy.

(b) Disproportionation. The reaction of **6** with an equimolar amount of indium(I) chloride results in the immediate deposition of indium metal upon mixing of the reagents, even at $-80^\circ C$. For comparison, the equivalent reaction was carried out using the dilithio *bam* $Li_2[PhB(NDipp)_2]$ and similar observations were made. After removal of indium metal by filtration, the isolated solid was determined by 1H NMR spectroscopy to be the previously reported spirocyclic indium(III) complex **9**,³¹ confirming that disproportionation of the initially formed *bam*In(I) complex had occurred (Scheme 3). It seems reasonable to suggest that a similar disproportionation takes place in the reaction of **6** with $InCl$. However, attempts to grow X-ray crystals of the product of this reaction were unsuccessful.

(c) Metathesis. In a few cases simple metathesis occurred in the reactions of **6** with p-block or group 12 element halides. For example, the reactions of **6** with $GeCl_2 \cdot dioxane$, $MgCl_2$, and $ZnCl_2$ proceeded cleanly to give products that are tentatively identified as $\{Ge[^iPr_2NB(NDipp)_2]\}_2 \cdot dioxane$ (**10**) and $M(THF)_x[^iPr_2NB(NDipp)_2]$ (**11**, $M = Mg$; **12**, $M = Zn$) on the basis of their NMR spectra. The 1H NMR data for the two types of isopropyl groups in the new *bog* complexes (**10**, $M = Ge$; **11**, $M = Mg$; **12**, $M = Zn$) are compared with those of **5** and **6** in Table 4. From these data it is clear that the CH_3 and CH resonances of the isopropyl groups and the CH_3 resonances of the Dipp groups in **10–12** are significantly shifted with respect to those in **5**; consequently, the presence of small amounts of **5** in the reaction products is readily detected. Unfortunately, the attempted separation of $LiCl$ from these products using non-coordinating solvents, for example, toluene and hexane, invariably resulted in the formation of some of the diprotonated derivative **5**. This observation is surprising in view of the lack of decomposition of the dilithio derivative **6** in toluene or hexane.

The complexes **10**, **11**, and **12** all show broad singlets in the ^{11}B NMR spectra at δ 28.0, 23.2, and 25.2, respectively, cf. δ 22.8 for the dilithio derivative **6**. A distinct downfield shift in these resonances is evident upon replacement of an

(27) Weber, L.; Rausch, A.; Wartig, H. B.; Stammler, H.-G.; Neumann, B. *Eur. J. Inorg. Chem.* **2002**, 2438.

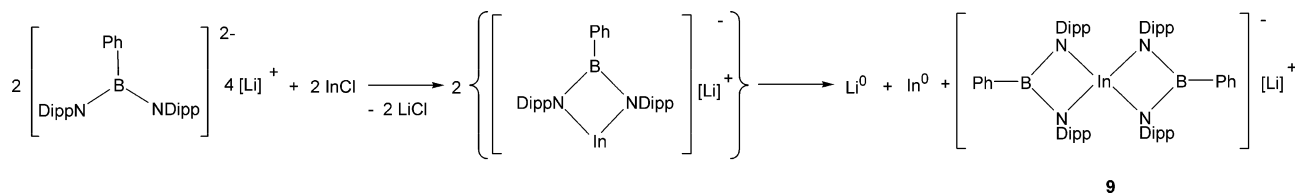
(28) Fußstetter, H.; Nöth, H. *Chem. Ber.* **1979**, *112*, 3672.

(29) Heine, A.; Fest, D.; Stalke, D.; Habben, C. D.; Meller, A.; Sheldrick, G. M. *J. Chem. Soc., Chem. Commun.* **1990**, 742.

(30) Manke, D. R.; Nocera, D. G. *Polyhedron* **2006**, *25*, 493.

(31) Chivers, T.; Fedorchuk, C.; Schatte, G.; Parvez, M. *Inorg. Chem.* **2003**, *42*, 2084.

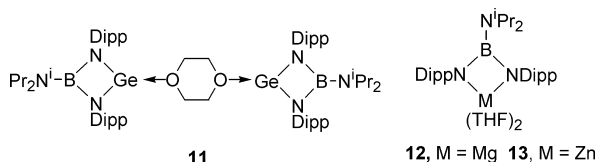
Scheme 3

**Table 4.** ^1H NMR Data (in ppm) for the Isopropyl Groups in **5**, **6**, and **10–12** (in THF- d_6)

	(5)	(6)	(10)	(11)	(12)
$-\text{CH}(\text{CH}_3)_2$ of Dipp groups	3.61	3.84	3.80	4.15	4.15
$-\text{CH}(\text{CH}_3)_2$ of $-\text{N}^i\text{Pr}_2$ groups	3.25	3.65	3.26	3.43	3.30
$-\text{CH}(\text{CH}_3)_2$ of Dipp groups	1.22, 1.16	1.20, 1.07	1.30, 1.16	1.18, 1.09	1.21, 1.13
$-\text{CH}(\text{CH}_3)_2$ of N^iPr_2 groups	1.12	0.92	0.86	0.76	0.76

electropositive metal (Li or Mg) by zinc or germanium.

The integration of the ^1H NMR resonances was used to estimate the extent of solvation in the complex $\{\text{Ge}[\text{Pr}_2\text{NB}(\text{NDipp})_2]\}_2 \cdot \text{dioxane}$ (**11**) and, on this basis, a structure in which the dioxane ligand bridges the two germanium centers is proposed. Coordinated THF resonances were also evident in the ^1H NMR spectra of the magnesium and zinc complexes $\text{M}(\text{THF})_x[\text{Pr}_2\text{NB}(\text{NDipp})_2]$ (**12**, $\text{M} = \text{Mg}$; **13**, $\text{M} = \text{Zn}$); the value of x is most likely 2 to complete the tetrahedral coordination sphere at these metals. Attempted crystallizations of **12** and **13** in the presence of coordinating ligands such as tetramethylethylenediamine (TMEDA) or PPh_3 gave either glassy non-crystalline materials or decomposition to **5**.



Conclusion

We have developed a high yield synthesis of the first stable dilithio *bog*, $\{\text{Li}_2[\text{Pr}_2\text{NB}(\text{NDipp})_2]\}_2$, which adopts a dimeric cluster structure similar to those of dilithio *bam*'s in the solid state. A comparison of the reactions of this new dilithio *bog* and those of dilithio *bam*'s with selected p-block and Group

12 metal halides reveals that the *bog* ligand is a much stronger reducing agent, presumably as a result of the electron-donating influence of the diisopropylamino substituent on boron. Consequently, the formation of a metal is frequently observed in attempted metathetical reactions. In some cases, for example, InCl , metal formation may result from disproportionation of the initial product rather than direct reduction. Metathesis does occur cleanly in some cases, for example, with MgCl_2 , ZnCl_2 , and GeCl_2 , but the characterization of the resulting *bog* complexes was limited to multinuclear NMR spectra because, in contrast to the dilithio derivative $\{\text{Li}_2[\text{Pr}_2\text{NB}(\text{NDipp})_2]\}_2$, the complexes of these divalent metals show a propensity to form $\text{Pr}_2\text{NB}(\text{NHDipp})_2$ in non-coordinating solvents. Modification of the reducing ability of the *bog* ligand by replacement of the diisopropyl amino substituent with weaker π -donating amino groups is under investigation.

Acknowledgment. The authors gratefully acknowledge financial support from the Natural Sciences and Engineering Council (Canada) and the Alberta Ingenuity Fund (A.M.C).

Supporting Information Available: X-ray crystallographic files in CIF format. This material is available free of charge via the Internet at <http://pubs.acs.org>.

IC801336T